Resonant electron–optical-phonon interactions for impurities in GaAs and GaAs/$Al_xGa_{1-x}As$ quantum wells and superlattices

J.-P. Cheng
Department of Physics and Astronomy, State University of New York at Buffalo, Buffalo, New York 14260 and Francis Bitter National Magnet Laboratory, Massachusetts Institute of Technology, Cambridge, Massachusetts 02139

B. D. McCombe*
Department of Physics and Astronomy, State University of New York at Buffalo, Buffalo, New York 14260

G. Brozak†
Francis Bitter National Magnet Laboratory, Massachusetts Institute of Technology, Cambridge, Massachusetts 02139

W. Schaff
Department of Electrical Engineering, Cornell University, Ithaca, New York 14853
(Received 2 August 1993)

A systematic experimental study of confinement effects on the strength of electron–optical-phonon interactions is presented. The hydrogenic $1s$-$2p_{+1}$ transition of shallow donors in bulk GaAs and GaAs/$Al_xGa_{1-x}As$ multiple quantum wells (MQW) and superlattices has been tuned through resonances with the GaAs optical phonons by magnetic fields up to 23.5 T and followed with far-infrared photoconductivity spectroscopy. Extremely large and asymmetric interaction gaps have been observed in both two-level and three-level resonance regions for small-well-width (125 Å) MQW samples. These gaps decrease systematically as the well width increases, approaching the bulk limit for the largest-well-width (450 Å) sample. For the superlattice sample (80-Å well and 9-Å barrier), the interaction is stronger than that for bulk, but much smaller than that for the MQW samples with comparable well width. Results are consistent with enhancement of the interaction as confinement progresses from three dimensions to two dimensions and demonstrate that the extent of the electronic wave function is the most important factor determining the interaction strength. Other phonon modes (interface phonons) may also contribute to the enhanced interaction for small-well-width samples. The $1s$-$3p_{+1}$ transition was also used to study the resonant polaron effects for strong-confinement MQW samples; results are consistent with those from the $1s$-$2p_{+1}$ transition.

I. INTRODUCTION

The interaction of an electron with longitudinal-optical (LO) phonons (polaron) is an important mechanism affecting electric transport properties in polar semiconductors. Within the framework of the Fröhlich formulation,[1] combined with the later development of quantum field calculations,[2] the problem has been extensively studied and is quantitatively well understood for three-dimensional (3D) bulk materials.[3] Recently, the electron-optical-phonon interaction in quasi-two-dimensional (2D) confined systems has attracted considerable attention due to its fundamental importance in carrier relaxation under hot-electron conditions. By comparison with bulk material, the layered nanostructures are much more complicated and less clear due to the effects of confinement on the electronic states[4–6] *and* to modifications of the bulk optical-phonon modes.[7–9] Initial theoretical calculations[4–6] made use of the Fröhlich interaction Hamiltonian with bulk phonon modes, and the 3D electronic states were replaced by appropriate quasi-2D states. Within this framework an enhanced polaron effect was predicted for systems with reduced dimensionality. However, some assumptions inherent to this treatment, such as the continuum lattice approximation and dispersionless phonons, may not be appropriate to the layered structures. More realistic phonon modes, including confined optical phonons and interface phonons, were observed by several groups[10–13] using Raman-scattering techniques. Theoretical studies concerned with these new lattice vibration excitations have been carried out in both macroscopic dielectric continuum models and microscopic models.[9,12–15] When these phonon modes are used for the electron-phonon interaction calculations, the behavior is very different from the results employing 3D phonons, and the conclusions are quite controversial.[16–19]

Several early cyclotron resonance (CR) experiments on degenerate quasi-2D electron systems have led to somewhat confusing results for the magnitude of the interaction; both enhanced and reduced polaron effects have been reported.[20,21] These apparent contradictions were later explained by screening[22,23] and occupation effects,[4] and recent CR measurements[24] have demonstrated that the interaction magnitude is indeed reduced with increasing electron density in single heterostructures.

To avoid the complications of screening and occupation effects, the present experiments have been carried

out on an alternative quasi-2D, but inherently single-particle, system—shallow donors confined in multiple-quantum-well (MQW) structures. Early work on this system was limited to the field and energy regions where essentially only the lowest branch of the resonant splitting can be clearly observed when the intraimpurity $1s$-$2p_{+1}$ transition tuned by a magnetic field approaches the GaAs phonons.[25,26] One of these studies[26] showed a large sublinear deviation of the lower branch and a rapid decrease of intensity of the transition at energies and magnetic fields well below the resonance with the bulk zone-center (Γ-point) LO phonon. To explain this "pinning" behavior, an unrealistically large Fröhlich coupling constant was required. With an enhanced signal-to-noise ratio and better resolution, we have recently extended the earlier measurements throughout both the so-called two-level and three-level resonance regions. Although no apparent "pinning" behavior can be seen, extremely large and asymmetric [with respect to GaAs LO (Γ) phonons] "interaction" gaps in the resonant energy region were observed.[27] The data can be fitted reasonably well by a calculation that includes both electron–interface-phonon and electron–confined-LO-phonon interactions.[28] On the other hand, other calculations have shown that the interface-phonon effect decays rapidly as the well width increases.[29] At the well width of the sample used in the experiment, the bulk LO phonon provides a reasonable approximation.[30] A systematic study of the well-width dependence is crucial in achieving a detailed understanding of the polaron problem in confined structures. Comparisons of results from MQW structures with those from bulk GaAs and narrow-barrier superlattices are also important in comprehending the role of confinement on the phonon modes and the relevance of these modifications to the interpretation of various optical and electronic transport phenomena.

In this paper we describe detailed far-infrared (FIR) magnetospectroscopic studies of the well-width dependence of impurity-bound magnetopolarons in several GaAs/$Al_xGa_{1-x}As$ MQW structures with well widths between 125 and 450 Å. A bulk GaAs sample and a superlattice sample with an 80-Å well and a 9-Å barrier were also investigated to provide base lines for comparison for different purposes. Photoconductivity has been used to follow the $1s$-$2p_{+1}$ (or $1s$-$3p_{+1}$) hydrogenic donor transition for well-center donors which was tuned through the resonant regions with GaAs optical phonons by magnetic fields up to 23.5 T. The systematic decreases of the "interaction" gaps and sublinear deviations with increasing well width for the MQW structures are taken to be evidence for an increased electron-phonon interaction with increasing confinement, and possibly an indication of the increasing role played by interface-phonon modes for the narrower well samples. Combined with the results from superlattice and bulk GaAs samples, these results demonstrate that the extent of the electronic wave function is the most important factor determining the interaction strength.

In Sec. II a brief outline of the relevant theoretical background and the conditions necessary for achieving two-level and three-level resonant interactions is presented. Experimental details are provided in Sec. III, followed by a description of the experimental results in Sec. IV. A discussion of these results and other complications is given in Sec. V, and finally a brief summary and conclusions are presented in Sec. VI.

II. BACKGROUND

The Fröhlich Hamiltonian for the electron–polar-optical-phonon interaction in bulk material can be written as[1]

$$H_{ep}=\sum_{\mathbf{q}} V_{\mathbf{q}}\exp(i\mathbf{q}\cdot\mathbf{r})\{a_{\mathbf{q}}-a^{\dagger}_{-\mathbf{q}}\} , \tag{1}$$

with

$$V_{\mathbf{q}}^2=\frac{4\pi\alpha\hbar}{\Omega q^2}(2m^*)^{-1/2}(\hbar\omega_{\mathrm{LO}})^{3/2} , \tag{2}$$

where $a^{\dagger}_{\mathbf{q}}$ ($a_{\mathbf{q}}$) is the creation (annihilation) operator of a LO phonon with wave vector $\mathbf{q}$ and frequency ω_{LO}. m^* and $\mathbf{r}$ are the effective (band-edge) mass and the position of the electron, respectively. Ω is the crystal volume, and α is the dimensionless Fröhlich coupling constant, which can be determined from the static and high-frequency dielectric constants and the effective mass [the accepted value for GaAs is $\alpha=0.068$ (Ref. 31)].

The self-energy correction ΔE and renormalized polaron effective mass m_p^* can be calculated in Rayleigh-Schrödinger perturbation theory (RSPT). The first-order energy correction vanishes because each term in H_{ep} contains only a single creation or annihilation operator for phonons. The second-order energy correction is

$$\Delta E_n=\sum_m \frac{\langle n|H_{ep}|m\rangle\langle m|H_{ep}|n\rangle}{E_n-E_m} , \tag{3}$$

where $|n\rangle$ denotes an eigenstate of the noninteracting Hamiltonian, including both electron *and* phonon states (but no coupling between them), and the sum is over a complete set of intermediate states. For a free electron in bulk material, the total energy including correction is[1]

$$\begin{aligned} E(\mathbf{k})&=-\alpha\hbar\omega_{\mathrm{LO}}+(1-\alpha/6)(\hbar\mathbf{k})^2/2m^* \\ &\approx-\alpha\hbar\omega_{\mathrm{LO}}+(\hbar\mathbf{k})^2/2m_p^* , \end{aligned} \tag{4}$$

where $1/m_p^*=(1-\alpha/6)/m^*$, or $m_p^*\approx m^*(1+\alpha/6)$, when α is small. The electron–LO-phonon interaction lowers the total energy and increases the effective mass of the quasiparticle.

The dynamical behavior of an electron in a quasi-2D system is qualitatively different from that in a 3D system due to the confinement, which leads to quantized energy levels (subband structure) for motion in the confinement direction. A straightforward approach to the calculation of the polaron effect in such a system is to use the Fröhlich 3D interaction Hamiltonian H_{ep} of Eqs. (1) and (2) and replace the 3D electronic states in $|m\rangle$ in the matrix elements, e.g., in Eq. (3), by appropriately modified quasi-2D electronic states. For a free strictly 2D electron, this procedure yields[5]

$$E(\boldsymbol{\kappa})=-(\pi/2)\alpha\hbar\omega_{\mathrm{LO}}+(\hbar\boldsymbol{\kappa})^2/2m_p^* , \tag{5}$$

with $m_p^* \approx m^*(1+\pi\alpha/8)$ and κ the two-dimensional wave vector. In this simple formation the polaron effect is enhanced by removing one electronic degree of freedom (hence, the restriction on the momentum conservation along the direction of confinement); the self-energy correction is increased by a factor of $\pi/2$, and the quasiparticle mass correction is increased by a factor of $3\pi/4$.

This simple theoretical treatment, however, may not be adequate for some quasi-2D systems, since the lattice vibrations are also modified in a layered structure with different materials, as in MQW's or superlattices. The bulk phonon modes in this case should be replaced by confined and interface-phonon modes, both of which can interact with charged carriers since they produce associated long-wavelength polarization fields.[15]

Another feature inherent to superlattices is the possibility of zone-folding effects. When the LO-phonon-dispersion curves of the two alternating materials which form the superlattice overlap, or when the thickness of one material is very small so that the vibrations in the adjacent layers can have a phase correlation, LO phonons can propagate throughout the whole structure along the growth direction. The new periodicity of the superlattice results in a new reduced "mini" Brillouin zone. The original bulk phonon modes having large wave vector along the growth direction can now be folded back into the small-wave-vector region of the first minizone. At present it is not clear how this zone folding affects the electron-phonon interaction, or indeed if there is enough coherence of these propagating phonons to permit the effects of zone folding to be seen in the electron-phonon interaction.

For many polar semiconductors the electron–LO-phonon interaction is sufficiently small ($\alpha \ll 1$) that the self-energy correction and effective-mass enhancement given by Eqs. (4) and (5) are very difficult to observe experimentally. From Eq. (3) it is clear that there will be a large resonant enhancement when E_n approaches E_m. To avoid the divergence in Eq. (3) at resonance, other calculational methods, such as Wigner-Brillouin perturbation theory (WBPT), must be employed. In WBPT, Eq. (3) is modified by replacing the denominator by the "self-consistent" energy denominator $(E_n + \Delta E_n - E_m)$. Such an approach leads to a resonant splitting of the electronic states into two branches when the electronic energy separation is tuned through the energy (energies) of the interacting phonons. In principle, the coupling strength can be obtained directly from the splitting of the two branches at resonance.

Optical resonant polaron experiments can be divided into two general classes according to the number of electronic levels involved. In the simplest situation only two electronic energy levels participate (the two-level process). In this case, as shown in Fig. 1 (Two-Level), the electronic energy separation, the optical-phonon energy, and the probing light photon energy are identical at resonance. This may lead to experimental difficulties since polar semiconductors are essentially opaque in the energy region between TO and LO phonon energies, i.e., the reststrahlen band; hence the lower branch of resonant splitting is masked in the vicinity of the optical-phonon energies. These difficulties can be partially circumvented by using very thin samples or sensitive photoconductivity techniques. The best way to avoid such problems is to make use of a three-level arrangement when possible, as shown schematically in Fig. 1 (Three-Level). Electronic states $|2\rangle$ and $|3\rangle$ are coupled via the emission or absorption of an optical phonon, so that at resonance the energy difference between them is equal to the optical-phonon energy. Instead of monitoring the optical transition between states $|2\rangle$ and $|3\rangle$ as in the two-level experiment, one probes the transition between states $|1\rangle$ and $|3\rangle$. Thus the photon energy is larger (or smaller, depending on the relative positions of E_1 and E_2) than the optical-phonon energy, and is thus free from strong lattice absorption and reflection. In the present experiments the electronic states involved in the two-level process are the confined hydrogenic impurity levels $1s$ and $2p_{+1}$, the separation between which can be tuned into resonance with the LO phonons of GaAs by magnetic fields between 15 and 19 T, depending on well width. In the three-level process, states $|1\rangle$ and $|3\rangle$ are the $1s$ and $2p_{+1}$ hydrogenic levels, while state $|2\rangle$ is, e.g., the $2p_{-1}$ level. The energy separation between $2p_{+1}$ and $2p_{-1}$ (the cyclotron resonance energy) can be tuned into resonance for this three-level process by magnetic fields between 20 and 23 T.

III. EXPERIMENT

All samples used in these studies were grown by molecular-beam epitaxy (MBE). The $GaAs/Al_xGa_{1-x}As$ MQW samples (samples 1–3) were doped with Si donors at the well centers (central $\frac{1}{3}$): Sample 1: 125-Å well, $x=0.3$; sample 2: 210-Å well, $x=0.3$; sample 3: 450-Å well, $x=0.23$. The doping concentration is $1\times10^{16}/cm^3$ for samples 1 and 2, and $5\times10^{15}/cm^3$ for sample 3. All these MQW samples have the same barrier width, 125 Å. The bulk GaAs sample (sample 4) is a 10-μm epitaxial layer doped with Si at $2\times10^{14}/cm^3$ on an undoped GaAs buffer layer. Sample 5, the superlattice sample, consists of 40 periods of 80-Å GaAs wells separated by 9-Å $Al_{0.3}Ga_{0.7}As$ barriers, and each of the wells was atomic planar (δ) doped at the center with Si donors at $10^{10}/cm^2$. The superlattice or MQW structures

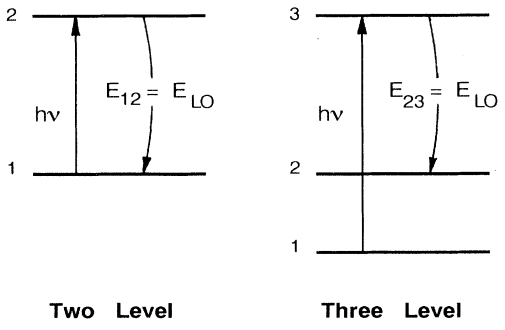

FIG. 1. Two-level and three-level resonant polaron processes. The probing photon energy is $h\nu$. For the two-level process, $h\nu = E_{LO}$. For the three-level process, $h\nu \neq E_{LO}$.

TABLE I. Summary of sample characteristics used in this experiment. The doping positions are central $\frac{1}{3}$ of the wells for samples 1–3 and a planarly δ doping for sample 5.

Sample	GaAs well width	$Al_xGa_{1-x}As$ barrier width	Al composition (x)	Doping density	Repetition
1	125 Å	125 Å	0.3	$1\times10^{16}/cm^3$	30
2	210 Å	125 Å	0.3	$1\times10^{16}/cm^3$	20
3	450 Å	125 Å	0.23	$5\times10^{15}/cm^3$	30
4	10 μm (bulk)			$2\times10^{14}/cm^3$	
5	80 Å	9 Å	0.3	$1\times10^{10}/cm^2$	40

were sandwiched between two thick (1500–2000 Å) $Al_xGa_{1-x}As$ cladding layers, and the whole structure was grown on a GaAs buffer layer on a semi-insulating GaAs substrate and capped by a ~100-Å GaAs layer. A summary of important parameters for all samples is listed in Table I.

The photoconductivity of the MQW samples and the superlattice sample was monitored by the capacitive coupling technique.[32] Two semitransparent chromium films separated by a small gap were evaporated on the top surface of the samples, acting as electrodes. The top AlGaAs cladding layer acts essentially as an insulator at low temperature, and the GaAs wells, due to photothermal ionization of doped impurities, appear as a set of parallel photosensitive resistors. A low-frequency (~100 Hz) ac voltage was applied between the two film electrodes coupled capacitively to the resistively conducting quantum-well plates, and the ac current through the sample was detected by a current-sensitive preamplifier and a lock-in amplifier. For the GaAs bulk sample Ohmic contacts were made on the thick epitaxial layer by indium diffusion, and the photoconductivity signal was measured by standard techniques.

Far-infrared magneto-optical spectra were obtained with Fourier-transform spectrometers in conjunction with a 9-T superconducting magnet or a 23-T Bitter magnet. The FIR output of the spectrometers was guided by light pipes and condensing-cone optics to the sample-detector assembly (the detector was used for alignment purposes). A thin cold black polyethylene film was placed in front of the sample as a optical low-pass filter. All data were taken at liquid-helium temperatures in the Faraday geometry (magnetic field parallel to the propagation direction of FIR light and normal to the sample surfaces).

IV. RESULTS

A. Bulk GaAs sample

In order to obtain reliable conclusions for the confinement effects on electron-phonon interactions in quasi-2D systems, reference data on bulk material for comparison are very important. Cyclotron resonance measurements have been used to study the resonant polarons in bulk GaAs.[33] However, for intraimpurity transitions in GaAs, we could not find existing experimental data covering the whole resonant region. We thus believe that the data reported here are the most complete set for impurity-bound resonant polarons in bulk GaAs. Aside from providing a reference for comparison purposes, they are interesting in their own right. For example, the Fröhlich coupling constant for bulk GaAs can be obtained by comparison of experimental results with theoretical calculations.[31]

In Fig. 2 we show the photoconductivity spectra of the impurity $1s$-$2p_{+1}$ transition in the resonant polaron region for sample 4. Notice that the 18-T spectrum looks much noisier than the other spectra. This is due to the fact that the transition is very close to the reststrahlen band at this field and the photoresponse is substantially reduced; thus the vertical scale has been expanded for this spectrum for a clearer comparison. At low magnetic fields (not shown in the figure), there is no transition observable beyond the LO (Γ) phonon energy (296 cm^{-1} at low temperatures) in the spectra. The upper branch of the two-level resonant splitting starts to appear at about 15 T (a weak peak at 297 cm^{-1}). It grows in relative intensity at the expense of the lower branch (strong peaks

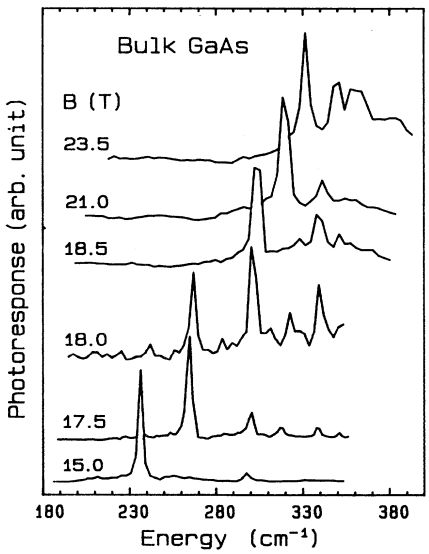

FIG. 2. Photoconductivity spectra for the $1s$-$2p_{+1}$ transition for the bulk GaAs sample at several magnetic fields in the resonant polaron region. The 18 T spectrum has been expanded for convenience of vision.

in the 15 and 17.5-T spectra) and moves up in transition energy with increasing magnetic field. At 18.5 T it becomes the strongest line in the spectrum, and the lower branch completely disappears. Meanwhile, several weak features appear at even higher energies, and increase in relative intensity as the field increases. These transitions have been attributed to the three-level resonant processes involving the $2p_{-1}$, $3d_{-2}$, $4f_{-3}$, and $2p_0$ states.[31]

The impurity transition energies as a function of magnetic field have been plotted in Fig. 3 (dots). The curves are calculations for the $1s$-$2p_{\pm 1}$ and $1s$-$2p_0$ transitions *without* electron–LO-phonon interaction.[34] The nonparabolicity corrections to the $1s$-$2p_0$ and $1s$-$2p_{-1}$ transitions are negligible since the transition energies change by only a small amount over the whole magnetic-field region studied. For the $1s$-$2p_{+1}$ transition the nonparabolicity correction has been taken into account by adding a corrected CR energy to the $1s$-$2p_{-1}$ transition. The resonant fields for the two-level process and the three-level process involving the $2p_{-1}$ state are about 19 and 22.5 T, where the unperturbed $1s$-$2p_{+1}$ transition crosses the LO-phonon energy E_{LO} and the energy of $[E(1s\text{-}2p_{-1})+E_{\mathrm{LO}}]$, respectively. At low fields the calculation fits the $1s$-$2p_{+1}$ transition data very well. Above 14 T the experimental data for the $1s$-$2p_{+1}$ transition clearly deviate from the unperturbed theoretical curve, and the transition disappears at the TO-phonon energy (the bottom of the reststrahlen band). The upper branch of the two-level resonant process appears above the LO-phonon energy, and it moves up with increasing magnetic field. At even higher energies, four resonant branches (three-level processes)—$2p_{-1}+\mathrm{LO}$, $3d_{-2}+\mathrm{LO}$, $4f_{-3}+\mathrm{LO}$, and $2p_0+\mathrm{LO}$—have been identified (see Ref. 31 for a detailed discussion). In addition, a nonresonant feature has also been observed (shown as the open squares in the figure), and the origin of this transition is not clear at present.

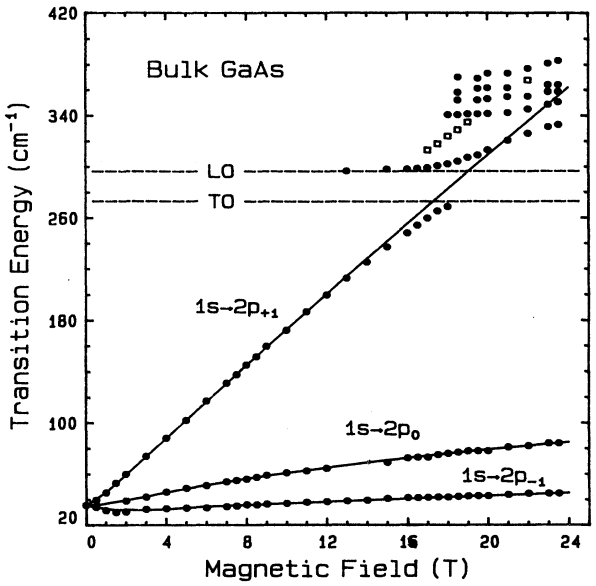

FIG. 3. Impurity transition energy vs magnetic field for the bulk GaAs sample. The dots are experimental data, and the curves are calculations without electron-phonon interaction (from Ref. 34). The open squares indicate the unidentified spectral feature.

B. Multiple-quantum-well samples

Photothermal ionization (photoconductivity) spectra of the $1s$-$2p_{+1}$ well-center (central $\frac{1}{3}$) impurity transition are shown in Fig. 4 for sample 1 (125-Å well width). At low magnetic fields [see 12-T spectrum in Fig. 4(a)], in contrast with the bulk results, the spectra exhibit a very asymmetrical line shape, i.e., a sharp peak at high energy with a tail extending ~ 30–40 cm^{-1} below. This is characteristic of the impurity distribution in the well. The sharp peak is due to impurities close to the well center (maximum in density of states), while the tail results from the off-center impurity distribution in the well.[35] As the field increases (above 12 T), the relative intensity of the sharp peak rapidly decreases, and near 14 T it becomes a weak shoulder which is difficult to resolve (indicated by arrows in the Figure). At fields above 14 T a sharp peak appears in the frequency region just above

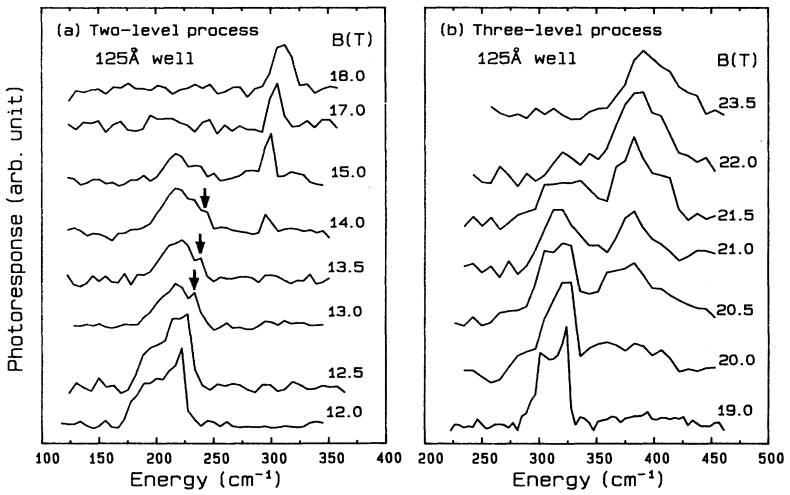

FIG. 4. Capacitively coupled photoconductivity spectra for the $1s$-$2p_{+1}$ transition for sample 1 at different magnetic fields: (a) Results in the two-level resonance region and (b) results in the three-level resonance region.

the GaAs LO (Γ) -phonon energy, which rapidly increases in intensity with increasing field. At still higher fields in the three-level resonance region [Fig. 4(b)] near 21 T, a splitting and intensity variation typical of an antilevel crossing similar to that observed near 14 T is clearly discernible, and it has been attributed to the interaction between the states $|2p_{+1},0\text{-phonon}\rangle$ and $|2p_{-1},1\text{-phonon}\rangle$. In comparison with the spectra of bulk GaAs in this field region, we cannot resolve the three-level resonance branches involving higher excited states. This is partly due to the fact that the confinement increases the energy separations of the impurity states (in fact, the $2p_0$ state, associated with the second subband, is well beyond the spectral region at this well width); hence a higher magnetic field is needed for the resonance condition. In addition, the complex line shape due to the impurity distribution in the well, the lower resolution, and the lower signal-to-noise ratio in comparison with the spectra of bulk GaAs also increase the difficulty in distinguishing these branches. Nevertheless, the spectra at highest fields show some structures (shoulders) at the high-energy side of the peak, which might be the indications of the three-level resonance branches involving the higher excited states associated with the first subband and $N=0$ Landau level, such as $3d_{-2}$ and $4f_{-3}$.[36]

The transition positions of Fig. 4 as a function of magnetic field are plotted in Fig. 5. For fields near 14 T, the positions of the "shoulders" on the high-energy side of the line profile, marked by arrows in Fig. 4(a), are plotted. The larger error bars for data points at the highest fields are partly due to the lower resolution. The dashed

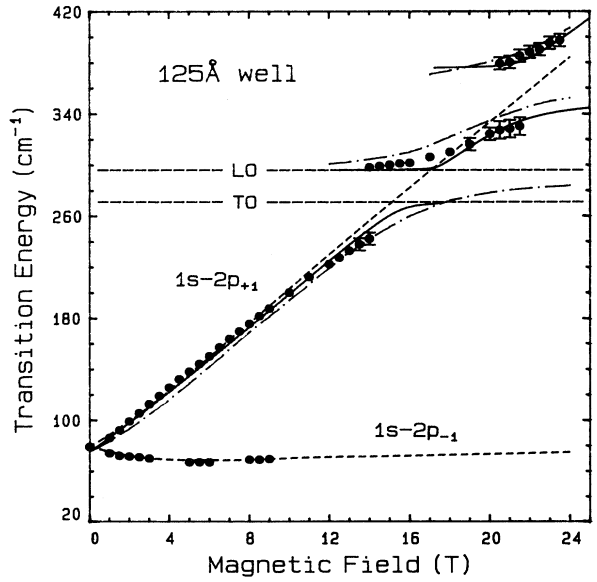

FIG. 5. Magnetic-field dependence of the impurity transition energies for sample 1. Dots, experimental data; dashed curves, calculated transition energies in the absence of interaction (Ref. 37); solid curves, calculation including electron-confined-LO-phonon and electron–interface-phonon interactions (Ref. 28); and dot-dashed curves, calculation with electron–(3D) LO-phonon interaction (Ref. 30).

curves are the calculations for the $1s$-$2p_{\pm1}$ transitions in the absence of polaron interaction;[37] a correction for nonparabolicity has been made to the calculation in a way similar to that discussed for the bulk sample, except that the CR mass in this case has to be corrected by both confinement and field effects. Three branches separated by two gaps are clearly observed. The lowest branch is depressed from the unperturbed curve for fields above 10 T and disappears completely in the region above 245 cm^{-1} (above 14.5 T), even though the slope in the energy-versus-field plot has not yet approached zero at this point. This energy, at which the line disappears, is well below (~ 50 cm^{-1}) the zone-center LO-phonon energy for GaAs, resulting in an extremely large and asymmetric (with respect to the GaAs LO phonon) "interaction" gap. The middle branch is actually the upper branch of the two-level process

$$E(2p_{+1})-E(1s)=E_{\mathrm{LO}} ,$$

and the lower branch of the three-level process

$$E(2p_{+1})-E(2p_{-1})=E_{\mathrm{LO}} ,$$

and thus represents the overall effect of these two resonant interactions. It moves up very slowly with field, crossing the unperturbed curve at approximately 17 T, and gradually approaches a frequency of about 330 cm^{-1}, again about 50 cm^{-1} below the frequency for pinning with a three-level process involving bulk GaAs LO (Γ) phonons. The upper branch for the three-level process begins at an energy of $E(1s\text{-}2p_{-1})+E_{\mathrm{LO}}$, increases in energy with the field, and approaches the unperturbed transition energy at the highest fields. It is apparent that the "interaction" gaps are very large and asymmetric, if it is assumed that the interaction takes place only with bulk zone-center LO phonons, and these anomalies in the resonant polaron regions strongly suggest that electrons are also interacting with other phonon modes that have lower energies than the bulk LO (Γ) phonons.

A calculation including electron–confined-LO-phonon and electron–interface-phonon interactions for a single QW with the same well width (125 Å) has been carried out,[28] and the result is shown by the solid curves in the Figure. The remarkable characteristic of the calculation is the lower branch pinning at the TO (Γ) phonon energy rather than the LO (Γ) phonon energy, which leads to a large and "asymmetric" interaction gap, in qualitative agreement with experimental data. On the other hand, another calculation using only GaAs bulk LO (Γ) phonons gives nearly equal agreement,[29] shown in Fig. 5 by the dot-dashed curves. The largest discrepancy occurs for the upper branch of the two-level resonance, where the experimental data are systematically below the calculated curve using only the bulk LO phonon, but higher than the calculation with both electron–confined-phonon and electron–interface-phonon interactions included. More detailed discussions will be given in Sec. V B. Based on these results, the well-width-dependent study is very important to understand quantitatively the magnitude of the resonant polaron interaction and to clarify the major contributions among different interaction mechanisms.

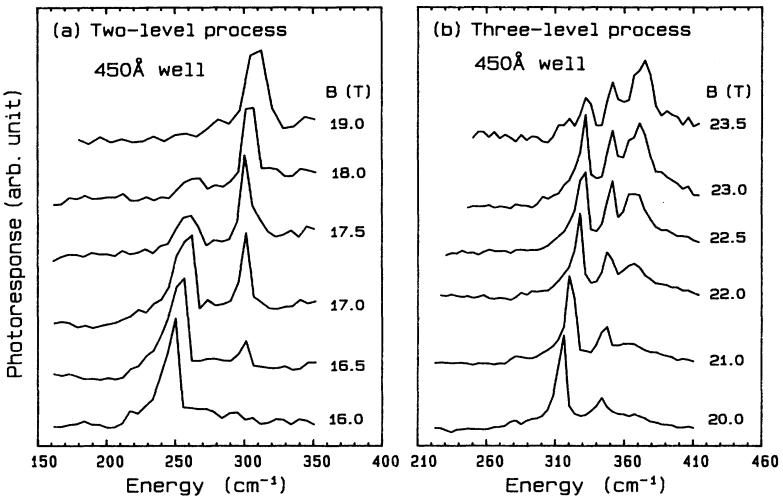

FIG. 6. Photoconductivity spectra of the $1s$-$2p_{+1}$ transition for sample 3 at several magnetic fields: (a) Two-level resonance region and (b) three-level resonance region.

Photoconductivity spectra of the $1s$-$2p_{+1}$ impurity transition for sample 3 (450-Å well width) are shown in Fig. 6 at various magnetic fields. In the two-level resonant energy region [Fig. 6(a)] the relative intensities of the two lines show typical antilevel crossing behavior, the lower branch disappearing at an energy slightly lower than the TO-phonon energy (the bottom of the reststrahlen band). This energy is *much higher* than that for sample 1. As the field is increased further, as we have discussed above, the $|2p_{+1},0\text{-phonon}\rangle$ state will cross the states $|2p_{-1},1\text{-phonon}\rangle$ and other higher excited states associated with the $N=0$ Landau level in a magnetic field, such as $|3d_{-2},1\text{-phonon}\rangle$ (ground subband) or $|2p_0,1\text{-phonon}\rangle$ (second subband). These three-level resonances have been clearly observed, as shown in Fig. 6(b), where the relative intensities of the three peaks show a typical interacting antilevel crossing behavior.

The transition energies as a function of magnetic field for this sample are plotted in Fig. 7 (dots). The solid curves are the unperturbed $1s$-$2p_{\pm1}$ transition energies based on the calculation of Ref. 37 with a correction for nonparabolicity. In addition to the two-level interaction gap, two separate three-level interaction gaps are observed at energies above the LO (Γ) phonon; one is due to the $2p_{-1}$ state and another possibly due to the $3d_{-2}$ state.[38] At magnetic fields between 14 and 17 T, the experimental data show clear depression from the unperturbed transition curve at energies below the TO (Γ) phonon, resulting in a large and asymmetric gap with respect to the crossing point of the unperturbed $1s$-$2p_{+1}$ transition with the LO (Γ) phonon energy. This apparent gap is smaller than that of sample 1, but comparable to that of bulk GaAs. Dielectric "artifacts" with optical response cannot be completely responsible for this sublinear behavior, as discussed below. In addition, experimental data taken on the bulk GaAs (sample 4) show *less* deviation from the unperturbed transition at even *higher* energies than those for sample 3 (the highest energy data point of the lowest branch is ~ 5 cm^{-1} below TO energy for sample 4 and ~ 8 cm^{-1} for sample 3), indicating that the slightly different behavior at the energies very close to the resonances between samples 3 and 4 cannot be explained merely by dielectric artifacts.

The $1s$-$2p_{+1}$ transition spectra for sample 2 (210-Å well width) show behavior in magnetic fields similar to that observed in samples 1 and 3. However, the magnitude of the "anomalies" in the resonant polaron region for sample 2 lies between those for samples 1 and 3 in a systematic way. For example, the apparent "interaction gaps" for this sample are larger than those for sample 3, but smaller than those for sample 1, and the energy at which the lower branch of the two-level process disappears is lower than for sample 3, but higher than for sample 1.

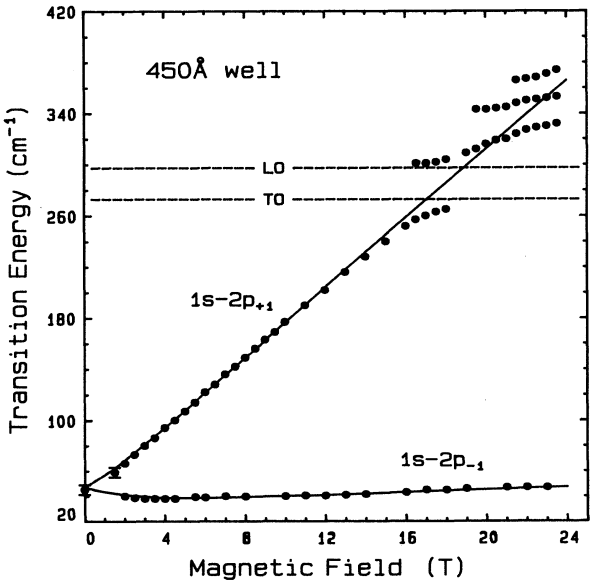

FIG. 7. Transition energies of $1s$-$2p_{\pm1}$ for sample 3 as a function of magnetic field. The circular dots are experimental results, and the solid lines are the calculated transition energy in the absence of electron–phonon interaction (Ref. 37).

C. Superlattice sample

The superlattice sample (sample 5) provides another reference for comparison with the MQW samples. Due to very thin barriers, the electronic wave function is much more extended than the narrow-well MQW sample (sample 1).[39] The confined-LO-phonon modes can become propagating modes in such thin-barrier superlattices;[40] hence the zone-folding effects on electron-phonon interactions can be explored. In addition, sample 5 has a smaller GaAs well width than sample 1, so it is expected that the interface-phonon modes may play a more important role. Detailed comparison of the results of superlattices with MQW's should yield more information concerning various mechanisms of electron-phonon interactions in the confined structures.

The capacitively coupled photoconductivity spectra for sample 5 at several magnetic fields in the resonant polaron region are shown in Fig. 8. At low magnetic fields, the $1s$-$2p_{+1}$ transition is a sharp, symmetric line due to the well-center planar δ doping for this sample. At about 15 T the upper branch of the two-level resonant process begins to appear at the LO (Γ) energy, increases in relative intensity, and moves to the higher energies as the field increases. With increasing magnetic field, the lower branch loses intensity and nearly disappears as it approaches the GaAs TO phonon (at about 19 T). However, at slightly higher fields, it reappears *inside* the reststrahlen band and finally vanishes at the highest magnetic fields. Due to a slightly larger CR mass for this superlattice sample,[41] the available field is not large enough to tune the $|2p_{+1}$,0-phonon$\rangle$ state to cross over the three-level resonant region with the $|2p_{-1}$,1-phonon$\rangle$ state. However, an indication of the three-level process can be seen at about 345 cm^{-1} in the spectra at the highest magnetic fields.

In Fig. 9 we display the magnetic-field dependence of the impurity transitions for this sample (solid squares) and compare the results with the bulk GaAs data (small open circles). The lower branch of the two-level resonance shows a clear sublinear behavior as it approaches the resonance. At the TO (Γ) energy, the transition energy shows a sudden jump, and it is pinned to ~285 cm^{-1} at higher fields. This might be due to the electron–interface-phonon interaction, since one of the interface-phonon modes is at GaAs TO-phonon energy in the long-wavelength limit, and the maximum of the density of states (interface-phonon modes) should lie somewhere between the GaAs TO- and LO-phonon energies in the middle of the reststrahlen band. On the other hand, the dielectric effect may also distort the spectra, and must be considered. We expect that the dielectric effect is small since the transition can appear inside the reststrahlen band. In comparison with the results of bulk GaAs, this sample shows a slightly larger sublinear behavior in the lower branch and a larger apparent interaction gap for the two-level resonance. The upper branch of the two-level process (or the lower branch of the three-level process) approaches an energy lower than that of the bulk GaAs sample in the highest field region, indicating a larger interaction splitting for the three-level resonant process, which is consistent with the results of the two-level resonant process. In comparison with the results for the MQW samples, this sample shows much *smaller* apparent "interaction gaps" than the narrow-well-width samples (samples 1 and 2), but comparable with the wide-well-width sample (sample 3).

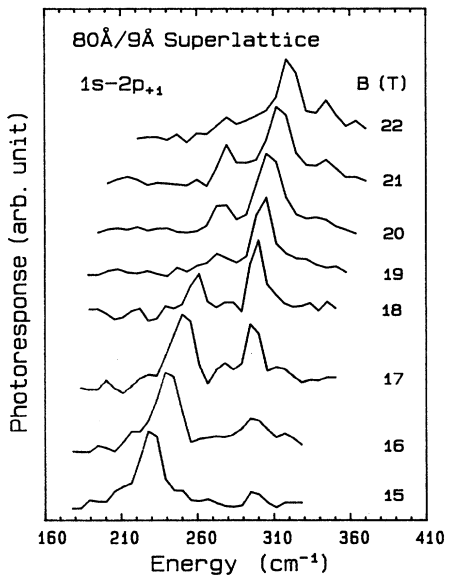

FIG. 8. Capacitively coupled photoconductivity spectra of the $1s$-$2p_{+1}$ transition for sample 5 at magnetic fields of the resonant interaction region. Notice that the transition can be observed *inside* the reststrahlen band between TO (273 cm^{-1}) and LO (296 cm^{-1}) phonon energies.

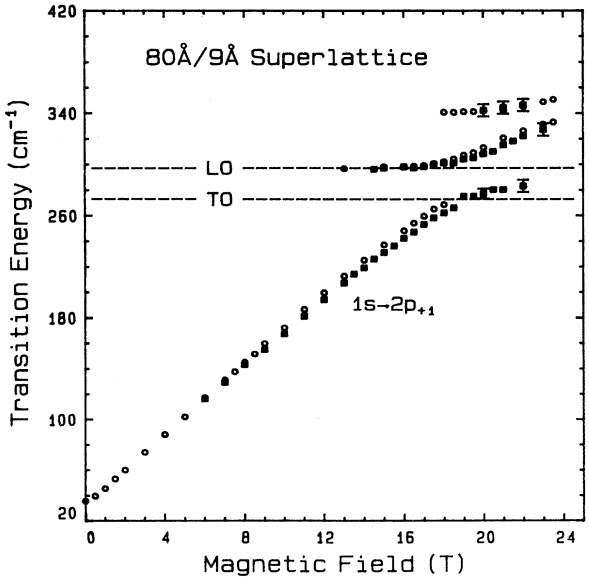

FIG. 9. The $1s$-$2p_{+1}$ transition energy vs magnetic field for sample 5 (solid squares). The experimental results for bulk GaAs (sample 4) are also plotted as open circles for comparison.

D. The $1s$-$3p_{+1}$ transition

As a complementary measurement, another shallow impurity transition, $1s$-$3p_{+1}$, has also been used to study the resonant magnetopolaron effects in strongly confined structures.[42] Figure 10 shows the capacitively coupled photoconductivity spectra for sample 1 (125-Å well width) at several magnetic fields. The dominant feature in the spectra is the $1s$-$2p_{+1}$ transition. A much weaker peak at higher energy has been identified as the $1s$-$3p_{+1}$ transition of the well-center impurities according to the electric dipole selection rules in this geometry and the low-field–high-field correspondences of hydrogenic impurity states in a strongly confined system.[36] With increasing magnetic field, this transition moves to higher energy approximately twice as fast as the $1s$-$2p_{+1}$ transition; thus it can be tuned through the resonance region at much lower magnetic field. When the field reaches about 6 T, the intensity of the $1s$-$3p_{+1}$ transition decreases dramatically and completely disappears at slightly higher fields. Meanwhile, a "new" line (the upper branch of the two-level resonance) appears at an energy slightly higher than the GaAs LO (Γ) phonon and moves to higher energies at even higher fields.[43] The three-level resonant process for the $1s$-$3p_{+1}$ transition,

$$E(3p_{+1})-E(2p_{-1})=E_{\mathrm{LO}}$$

should occur at ~ 11.5 T. At present, the measurements have been carried out only in a 9-T magnet, and the three-level resonance cannot be seen at this field.

A plot of the $1s$-$3p_{+1}$ transition energy versus magnetic field is presented in Fig. 11. The curve in the plot is a rough calculation for the transition energy without polaron interaction, obtained from[36]

$$E(1s\text{-}3p_{+1})=E(1s\text{-}2p_{-1})+2\hbar\omega_c+\Delta\ ,$$

where $E(1s\text{-}2p_{-1})$ is the $1s$-$2p_{-1}$ transition energy in QW calculated in Ref. 37, $\hbar\omega_c$ is the CR energy, and Δ is a parameter introduced to take into account the zero-field energy difference between $2p$ and $3p$. A nonparabolicity correction has been made to the CR energy. It is clear that the experimental data in the lower branch deviate to lower energies from the unperturbed transition at magnetic fields far from the resonant field (at which the unperturbed transition energy crosses the LO-phonon energy) and completely disappear around 245 cm^{-1}, well below the LO (Γ) -phonon energy, resulting in a very large and asymmetric "interaction" gap. These results are qualitatively the same as the results observed for the $1s$-$2p_{+1}$ transition in the two-level resonant polaron region (see Fig. 5).

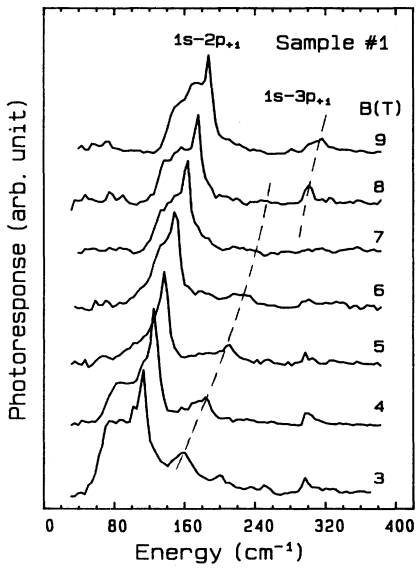

FIG. 10. Photoconductivity impurity transition spectra for sample 1 at several magnetic fields. The $1s$-$3p_{+1}$ transitions are highlighted by the dashed lines. The weak features at ~ 296 cm^{-1} in the low-magnetic-field (≤ 5 T) spectra are the LO-phonon responses, not the impurity transition.

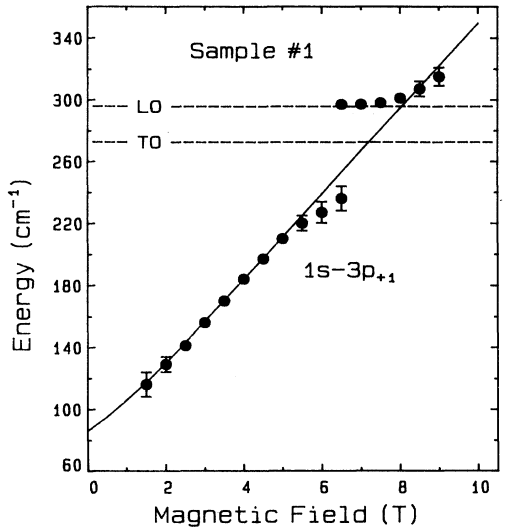

FIG. 11. Magnetic-field dependence of the $1s$-$3p_{+1}$ transition energy for sample 1. The curve is a rough fitting (see text) for the unperturbed impurity transition.

V. DISCUSSIONS

A. Well-width dependence

The results for MQW samples have clearly shown that the observed apparent interaction gaps in both two-level and three-level resonant interaction regions progressively decrease as the well width increases, and approach the bulk 3D limit for the large-well-width MQW sample (sample 3), indicating enhanced electron-phonon interactions in a confined system.

In Fig. 12 we compare the observed energy deviations from the calculated unperturbed transitions in the lowest branch by plotting the negative energy shift as a function of magnetic field measured from the resonant field, B_{res} [the field at which the unperturbed transition crosses the GaAs LO (Γ) energy]. Differences in nonparabolicity

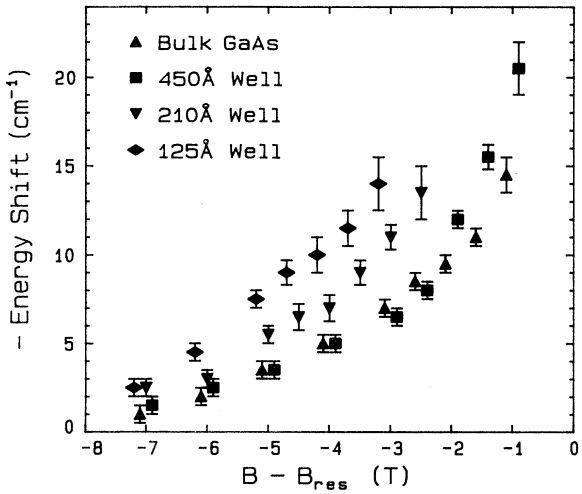

FIG. 12. Comparison of energy deviations from the unperturbed transition for the lowest branch for different well-width MQW samples and the bulk GaAs sample: $B_{res}=17.2$, 18.0, 18.9, and 19.1 T for samples 1, 2, 3, and 4, respectively.

corrections for different well widths have been taken into account in determining the unperturbed transition energies. There is no discernible difference between the 450 Å well-width sample and the bulk sample within the experimental error until the magnetic field is within ~ 1.5 T of B_{res}, where the data for the 450-Å well-width sample clearly show larger deviations than those for the bulk. As the well width decreases, the magnitude of the deviations increases systematically, indicating a stronger electron-phonon interaction for narrower-well-width samples, and consistent with the conclusion from the gap comparison.

The enhanced polaron effects in strongly confined structures can be attributed to two major mechanisms: one is electronic wave-function confinement, which leads to a larger phase space for the electron due to the fact that the translational symmetry (momentum conservation) is broken along the confinement direction; the second is the electron–interface-phonon interaction. Both mechanisms exhibit qualitatively similar dependence on the QW width, namely, the strength of the interaction increases with decreasing well width, as observed on the MQW samples in the present experiments. For the superlattice sample (sample 5), the results favor the former mechanism. The electronic wave function in the superlattice sample is much more extended than that in the narrow-well-width MQW samples (but less extended than that in the bulk sample) due to the thin barriers,[39] and we expect stronger interface-phonon effects in the superlattice due to the narrower wells in comparison with the MQW samples. The observed behavior for this sample, overall, is very similar to that of the bulk sample with slightly larger interactions, demonstrating that the electronic wave-function extent in the confined direction is the most important factor determining the strength of the resonant polaron interactions in confined structures in the well-width region studied.

B. Interface-phonon effects

The above conclusion does not exclude the possibility that the interface phonons play an important role for small-well-width samples, and, in fact, some detailed features in the results for sample 5 (the superlattice sample), such as the sudden jump of the transition energy at the TO phonon (the lower edge of the interface-phonon modes) and apparent pinning behavior *between* the TO and LO energies, might be a signature of electron–interface-phonon interaction. In addition, the asymmetry of the apparent gaps [with respect to the GaAs LO (Γ) phonon] observed for the narrow-well-width MQW samples strongly suggests that electrons interact with more than one set of phonon modes and that some contributions come from phonon modes *below* the LO-phonon energy.

A theoretical calculation for impurity-bound magnetopolarons in a quantum well has been carried out recently considering both electron–interface-phonon and electron–confined-LO-phonon interactions,[28] and the results for a 125-Å well-width QW has been plotted in Fig. 5 as the solid curves for comparison with the experimental data. Due to the interface-phonon dispersion, which forms a band between the TO- and LO-phonon energies,[11–15] a large interaction gap between TO and LO phonons has been predicted, which qualitatively agrees with experimental observation for narrow-well-width MQW samples,[28] and the calculation fits the data for sample 1 reasonably well. However, the calculations do not show how this gap changes as the well width changes. In principle, the electron–interface-phonon interaction should decrease rapidly as well width increases since the interface-phonon modes are confined to a narrow spatial region close to the interfaces, and the results of MQW samples are qualitatively consistent with this assertion. On the other hand, the electronic wave-function confinement will also lead to the same qualitative result in the well-width dependence. In fact, it is the most important factor determining the interaction strength, as discussed above; therefore, it is difficult to extract the contribution of the electron–interface-phonon coupling from present results without very accurate calculations with various interaction mechanisms.

In contrast to the above model calculation, a recent calculation[30] employing the 3D Fröhlich Hamiltonian (ignoring interface-phonon modes) agrees equally well with the experimental data for sample 1 (shown in Fig. 5 as the dot-dashed curves). Nonparabolicity corrections were claimed to be essential to fit the data. With this model calculation, the only "pinning" energies are those involving the bulk GaAs LO (Γ) phonon, and the resonant splitting should be centered about those energies, regardless of the sample structure; thus it is very difficult to understand the extremely asymmetric gaps observed for the narrow-well-width MQW samples, and more importantly, the systematic tendency for the lower branch of the two-level resonance to disappear at lower and lower energies (well below the LO and TO energies) as the confinement increases.

Due to many other complications (such as dielectric effects), the present data do not provide any clear evi-

dence for the electron–interface-phonon interaction, even though some features can be explained naturally by the interface-phonon effects. Detailed comparisons between the experimental data and theoretical calculations with different mechanisms are necessary in order to clarify this issue. Although the electron–(3D) LO-phonon interaction model with sufficiently accurate coupling constant α (Ref. 44) might be a good approximation for the large-well-width QW's, it has to be replaced by the electron–confined-LO-phonon and electron–interface-phonon interaction for sufficiently strong confinement structures, since those are the only proper phonon modes in such structures.

C. Dielectric effects

The dielectric function of a polar semiconductor diverges at the TO-phonon energy and becomes negative between TO and LO phonons; thus in optical measurements the spectroscopic line shape could be strongly distorted if the transition energy were very close to the phonons, leading to so-called dielectric artifacts. For multilayered structures, it could be even more serious due to the internal multiple-reflection interference of the light near the reststrahlen band; hence it is particularly important to study the dielectric response of FIR light for our samples in order to ensure that the data in the two-level resonant region are reliable.

A computer simulation for the transmission spectra, which are more sensitive to dielectric effects than the presently employed photoconductivity techniques, on typical MQW structures has been carried out.[45] Bulk dielectric functions appropriate to the lattice properties of the wells and barriers were used, and a Lorentzian electronic oscillator was taken to represent the impurity transition. The transfer matrix method[46] was used to couple the **E** field of the light between the adjacent layers, and the normalized transmission spectra were obtained by ratioing the transmitted spectrum *with* an impurity transition oscillator to the spectrum *without* the oscillator. Results have shown that the positions of the transmission minima will *not* deviate (<2 cm^{-1}) from the input transition energies until the minimum is very close to the TO phonon (within ~ 5 cm^{-1}), and there is *no* sudden vanishing of the absorption intensity (oscillator strength) in the energy region where the $1s$-$2p_{+1}$ transition disappears as observed in the experiment.[45] It is clear that dielectric effects alone cannot explain the observed anomalies in the resonant region for the narrow QW samples. However, it is worthwhile to point out that bulk dielectric properties may not be completely suitable for the nanostructures, since the lattice vibrations should be modified by the boundary conditions; hence the new phonon modes, such as the confined TO (LO) phonons and interface phonons in quasi-2D systems, should be used to calculate the dielectric functions or optical responses in nanostructures.

D. Zone-folding effect

Under certain conditions, such as very thin $Al_xGa_{1-x}As$ barriers and/or overlap of the GaAs LO-phonon-dispersion curve with the $Al_xGa_{1-x}As$ GaAs-like LO-phonon dispersion, the phonon modes may propagate along the superlattice direction. Very recently, the confined-to-propagating transition of LO phonons in $GaAs/Al_xGa_{1-x}As$ superlattices has been observed experimentally.[40] Results show that the transition depends on both the barrier width and the Al composition, x. In a propagating-LO-phonon superlattice, the original LO-phonon dispersion can be folded into a mini-Brillouin zone according to the superlattice period, and the electrons in the well thus might interact with the folded-zone-edge (X point) LO phonons at much lower energies [~ 250 cm^{-1} for GaAs LO (X) phonon] than with the LO (Γ) phonon. This assertion can provide a possible explanation for the anomalies observed on the narrow-well-width MQW samples—more specifically, the lower branch of the two-level resonance disappearing at the energy region near to the GaAs LO (X) phonon.[26] If this explanation is correct, we would expect much larger zone-folding effects for our thin-barrier superlattice sample (sample 5), since it is much easier for the LO phonon to propagate. Experimentally, we can follow the impurity transition up to the TO (Γ) -phonon energy without seeing any anomalous behavior (disappearing) in the transition intensities as such as those observed for the strongly confined MQW samples (see Figs. 8 and 9). This is the *opposite* of expectations based on zone folding. From the results of Ref. 40, we estimate that all of our MQW samples are in the confined-LO-phonon region, while the superlattice sample is in the propagating-LO-phonon region. These facts demonstrate that the electron–folded-LO-phonon interaction is very small and can be neglected in present investigation, contrary to earlier suggestions.[26]

VI. SUMMARY AND CONCLUSIONS

With no complications of screening and occupation effects, impurity-bound resonant magnetopolarons have been clearly observed in bulk GaAs, and in $GaAs/Al_xGa_{1-x}As$ superlattices and MQW's with different well widths for both two-level and three-level resonant interactions. For strongly confined MQW samples, the lower branches of the resonances show large deviation from the unperturbed transition and disappear at energies far below the GaAs LO (Γ) phonon, resulting in extremely large and asymmetric [with respect to GaAs LO (Γ) phonons] apparent "interaction" gaps. These gaps, as well as the sublinear deviations, decrease systematically as the well width increases and approach the 3D bulk limit for the widest well sample. These experimental facts clearly show that the electron-phonon interaction is enhanced by one-dimensional confinement. The superlattice sample shows a stronger interaction than the bulk, but much weaker interaction than the MQW samples with comparable well width, indicating that the most important factor for enhanced polaron interaction in quasi-2D systems is the electronic wave-function compression. The interface phonons may also contribute to this enhancement, particularly for the narrow-well-width samples, but a definite conclusion

would require detailed comparisons between the experimental results and theoretical calculations. The electron–folded-LO-phonon interactions and dielectric artifacts (with bulk dielectric properties) are not responsible for the anomalies observed on the narrow-well MQW samples based on our experimental facts and a computer simulation; however, a revised dielectric function including confined phonons and interface phonons for quasi-2D structures should be used in these investigations. Such an approach might provide an explanation for the vanishing of the transition intensity observed on the strongly confined samples in the resonant polaron region.

ACKNOWLEDGMENTS

Most of this work was carried out at the Francis Bitter National Magnet Laboratory; we are grateful to the staff, especially B. Brandt and L. Rubin, for assistance. J. P. C. and B. D. M. wish to thank J. Ralston and G. Wicks for expert sample growth of samples 1 and 2, and B. Shanabrook and S. Holmes for providing samples 3 and 4, respectively. We also acknowledge useful discussions with F. Peeters, J. Devreese, R. Chen, and D. L. Lin. This work was supported by ONR Grant No. N00014-89-J-1673.

---

*Visiting scientist, Francis Bitter National Magnet Laboratory.

†Present address: Radix-II, Oxon Hill, MD 20375.

[1]H. Fröhlich, Proc. R. Soc. London, Ser. A **160**, 230 (1937).

[2]R. P. Feynman, Phys. Rev. **84**, 108 (1951).

[3]See, e.g., *Polarons in Ionic Crystal and Polar Semiconductors*, edited by J. T. Devreese (North-Holland, Amsterdam, 1972).

[4]D. M. Larsen, Phys. Rev. B **30**, 4595 (1984).

[5]S. Das Sarma, Phys. Rev. B **27**, 2590 (1983); Phys. Rev. Lett. **52**, 859 (1984).

[6]F. M. Peeters and J. T. Devreese, Phys. Rev. B **31** 3689 (1985); F. M. Peeters, X. Wu, and J. T. Devreese, *ibid.* **33**, 4338 (1986).

[7]M. Cardona, Superlatt. Microstruct. **5**, 27 (1989).

[8]J. Menendez, J. Lumin. **44**, 285 (1989).

[9]T. Tsuchiya, H. Akera, and T. Ando, Phys. Rev. B **39**, 6025 (1989).

[10]B. Jusserand, D. Paquet, and A. Regreny, Phys. Rev. B **30**, 6245 (1984).

[11]A. K. Sood, J. Menendez, M. Cardona, and K. Ploog, Phys. Rev. Lett. **54**, 2111 (1985); **54**, 2115 (1985).

[12]C. Colvard, T. A. Gant, M. V. Klein, R. Merlin, R. Fischer, H. Morkoc, and A. C. Gossard, Phys. Rev. B **31**, 2080 (1985).

[13]A. K. Arora, A. K. Ramdas, M. R. Melloch, and N. Otsuka, Phys. Rev. B **36**, 1021 (1987).

[14]K. Huang and B. F. Zhu, Phys. Rev. B **38**, 2183 (1988); **38**, 13 377 (1988).

[15]R. Cheng, D. L. Lin, and T. F. George, Phys. Rev. B **41**, 1435 (1990).

[16]R. Lassnig, Phys. Rev. B **30**, 7132 (1984).

[17]N. Sawaki, J. Phys. C **19**, 4965 (1986).

[18]B. K. Ridley, Phys. Rev. B **39**, 5282 (1989); B. K. Ridley and M. Babiker, *ibid.* **43**, 9096 (1991).

[19]F. Comas, C. Trallero-Giner, and R. Riera, Phys. Rev. B **39**, 5907 (1989).

[20]M. Horst, U. Merkt, and J. P. Kotthaus, Phys. Rev. Lett. **50**, 754 (1983).

[21]W. Seidenbusch, G. Lindemann, R. Lassnig, J. Edlinger, and E. Gornik, Surf. Sci. **142**, 375 (1984).

[22]S. Das Sarma and B. A. Mason, Phys. Rev. B **31**, 5536 (1985).

[23]X. Wu, F. M. Peeters, and J. T. Devreese, Phys. Rev. B **34**, 2621 (1986).

[24]C. J. G. M. Langerak, J. Singleton, P. J. van der Wel, J. A. A. J. Perenboom, D. J. Barnes, R. J. Nicholas, M. A. Hopkins, and C. T. P. Foxon, Phys. Rev. B **38**, 13 133 (1988).

[25]S. Huant, W. Knap, G. Martinez, and B. Etienne, Europhys. Lett. **7**, 159 (1988).

[26]Y.-H. Chang, B. D. McCombe, J.-M. Mercy, A. A. Reeder, J. Ralston, and G. A. Wicks, Phys. Rev. Lett. **61**, 1408 (1988).

[27]J.-P. Cheng, B. D. McCombe, and G. Brozak, Phys. Rev. B **43**, 9324 (1991).

[28]D. L. Lin, R. Chen, and T. F. George, Phys. Rev. B **43**, 9328 (1991).

[29]G. Hai, F. M. Peeters, and J. T. Devreese, Phys. Rev. B **42**, 11 063 (1990).

[30]J. M. Shi, F. M. Peeters, and J. T. Devreese, Phys. Rev. B **44**, 5692 (1991).

[31]J.-P. Cheng, B. D. McCombe, J. M. Shi, F. M. Peeters, J. T. Devreese, Phys. Rev. B **48**, 7910 (1993).

[32]J.-M. Mercy, N. C. Jarosik, B. D. McCombe, J. Ralston, and G. Wicks, J. Vac. Sci. Technol. B **4**, 1011 (1986).

[33]See, e.g., H. Sigg, P. Wyder, and J. A. A. J. Perenboom, Phys. Rev. B **31**, 5253 (1985); G. Lindemann, R. Lassnig, W. Seidenbusch, and E. Gornik, *ibid.* **28**, 4693 (1983).

[34]P. C. Makado and N. C. McGill, J. Phys. C **19**, 873 (1986).

[35]See, e.g., N. C. Jarosik, B. D. McCombe, B. V. Shanabrook, J. Comas, J. Ralston, and G. Wicks, Phys. Rev. Lett. **54**, 1283 (1985).

[36]J.-P. Cheng and B. D. McCombe, Phys. Rev. B **42**, 7626 (1990).

[37]R. L. Greene and K. K. Bajaj, Phys. Rev. B **31**, 913 (1985).

[38]F. M. Peeters (private communication).

[39]N. Nguyen, J. Zang, R. Ranganathan, B. D. McCombe, and M. L. Rustgi, Phys. Rev. B **19**, 14 226 (1993).

[40]D.-S. Kim, A. Bouchalkha, J. M. Jacob, J. F. Zhou, J. J. Song, and J. F. Klem, Phys. Rev. Lett. **68**, 1002 (1992).

[41]R. Ranganathan, B. D. McCombe, Y. Zhang, N. Nguyen, M. Rustgi, and W. Schaff (unpublished).

[42]For large-well-width samples, the $3p_{+1}$ state may mix with other excited states in magnetic field, hence complicating the problem (see Ref. 36).

[43]The weak feature at $\sim 296\ \mathrm{cm}^{-1}$ in the spectra of low magnetic fields is the LO-phonon response to the photoconductivity, and it does not move with the field.

[44]The results of impurity-bound resonant polarons in bulk GaAs are presently being compared with accurate theoretical calculations with the value of α varied within the range permitted by uncertainties in the dielectric constants (see Ref. 31).

[45]J.-P. Cheng and B. D. McCombe, Phys. Rev. Lett. **62**, 1925 (1989).

[46]K. Karrai, S. Huant, G. Martinez, and L. C. Brunel, Solid State Commun. **66**, 355 (1988).